Transactions of the Korean Nuclear Society Autumn Meeting
Gyeongju, Korea, October 27-28, 2016

SAFETY INJECTION TANK PERFORMANCE ANALYSIS USING CFD

Jai Oan Cho [a], Yacine Addad [b], Jeong Ik Lee [a*], Yohanes Setiawan Nietiadi [a], Young Seok Bang[c], Seung Hun Yoo[c]
[a]*Department of Nuclear and Quantum Engineering, Korea Advanced Institute of Science and Technology (KAIST)*
[b]*Department of Nuclear Engineering, Khalifa University of Science, Technology & Research (KUSTAR)*
[c]*Department of Safety Evaluation, Korea Institute of Nuclear Safety (KINS)*
[*]*Corresponding author: jeongiklee@kaist.ac.kr*

1. Introduction

The Advanced Power Reactor(APR) 1400 is a pressurized water reactor (PWR) of 1400MWe. Just like many other water reactors, it has an emergency core cooling system (ECCS). One of the most important components in the ECCS is the safety injection tank (SIT). Inside the SIT, a fluidic device (FD) is installed, which passively controls the mass flow of the safety injection of the coolant, eliminating the need for low pressure safety injection pumps.

As passive safety mechanisms are emphasized nowadays, it has become more important to understand the flow structure and loss mechanism within the FD.

During the high flow mode, water level is higher than the stand pipe height. Hence, water flows into the vortex chamber of the FD from two ports, the supply port and the control port. Water from the two different nozzles collide and flows into the discharge pipe directly.

During the low flow mode, water level is lower than the stand pipe height, therefore, water can only flow into the vortex chamber through the control port. Therefore, the flow is directed to a tangential angle of the vortex chamber generating a vortex, resulting in a lower water flowrate supplied to the reactor core.

Most 1D system codes have used single or double k-factors to control the mass flow of SITs. However, in the real case, the k-factor is not a constant and mass flow is not constant. Moreover, as the water level drops, nitrogen may be entrained into the discharge pipe and then into the core. This may affect the core cooling capability and threaten the fuel integrity during LOCA situations. However, information on the nitrogen flow rate during discharge is very limited due to the associated experimental measurement difficulties, and these phenomena are hardly reflected in current 1D system codes. In the current study, a CFD analysis is presented which hopefully should allow obtaining a more realistic prediction of the SIT performance which can then be reflected on 1D system codes to simulate various accident scenarios.

Current Computational Fluid Dynamics (CFD) calculations have had limited success in predicting the fluid flow accurately. This study aims to find a better CFD prediction and more accurate modeling to predict the system performance during accident scenarios.

2. Methods

Over four million polygonal prism meshes were used with a quality threshold of 0.4. Base size was given as 10cm. To capture the flow inside the fluidic device, very fine meshes were needed. The mesh in the fluidic device has a base size 10% relative to the tank and 2.5% in certain areas. Cross section of the grid system can be seen in Fig.1. and Fig.2. Minimum face quality of 0.05 was given for the surface. 6 prism layers are used for the walls with a stretching factor of 1.08. The growth factor is given as 0.1 to reflect the gradual increase of mesh size in the boundary of volume control blocks. Maximum safe skewness angle of 75 degrees was given, while minimum unsafe skewness angle was 88 degrees.

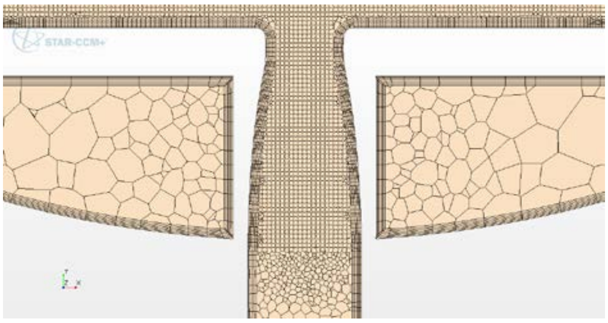

Fig.1. Grid system in discharge pipe

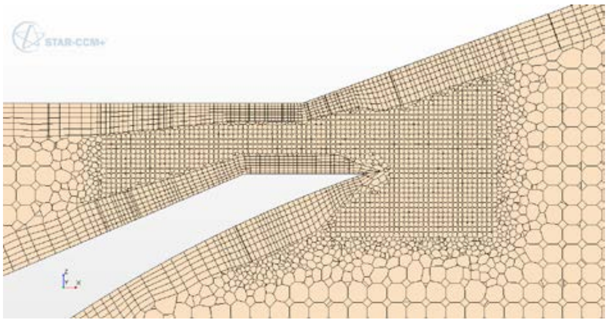

Fig.2. Grid system in Fluidic Device

Eulerian Multiphase model was used to model the water and nitrogen gas. VOF model was used to capture the free surface. Multiphase equation of state was calculated. Multiphase VOF-VOF interaction was calculated using a constant surface tension of 0.074. Segregated Flow model was selected along with the segregated multiphase temperature. The realizable K-ε model, with high y+ wall treatment was used for the implicit unsteady computation with a time step of 5.0E-6s. The under-relaxation factor of 0.7 was used for the segregated VOF and the turbulence model equations.

The computational domain initial condition was set by defining a hydrostatic pressure corresponding to the experimental set up. The initial temperature was set at 293K. The tank was given a constant thermal resistance and constant heat transfer coefficient by taking into account the tank thickness and material property. Constant ambient temperature of 293K was used along with convective boundary condition on the tank wall. Lastly, a pressure boundary of 1 bar and an appropriate constant loss coefficient was given at the end of the discharge pipe to account for the piping between the SIT and the core.

Continuity, momentum, energy, turbulent dissipation rate, and turbulent kinetic energy were monitored for convergence. Criteria was on 0.1 and the calculation proceeded once all values reached a residual below 0.1. Maximum inner iteration of 20 was given.

3. Results

The calculation is still running and the final results are expected to be presented in the conference. Nevertheless, we can still observe some interesting points. To compare the CFD result with the experiment result, the CFD result was also averaged for every 5s and interpolated. Although the initial states are different, Fig. 3 shows that the mass flow rate of the two tests converge at a certain value once the flow is fully developed. The results were normalized using the maximum flow rate of the experiment.

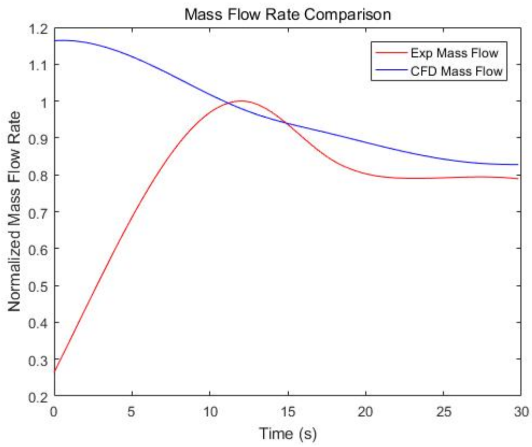

Fig.3. 15 bar Experiment and CFD Mass Flow Comparison

The K-factor should also be compared. As shown in Fig. 4, the two test results converge to a certain value. It takes around 10s for the valve to fully open and the flow to be fully developed. Therefore, we can clearly say that our CFD result is quite valid. The valve is opened over a few seconds in the experiment, so the K-factor starts with an extremely high value and converges very quickly. Fig. 4 is normalized using the minimum K-factor from the experiment.

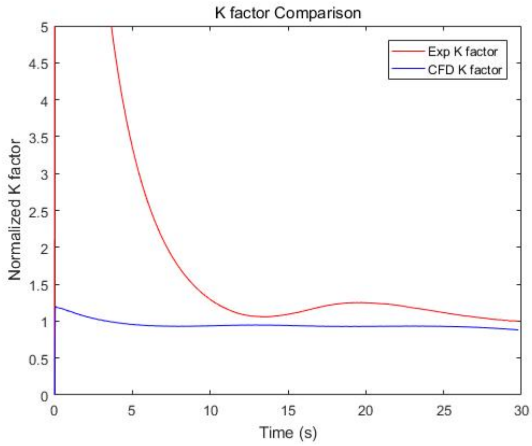

Fig.4. 15 bar Experiment and CFD K-Factor Comparison

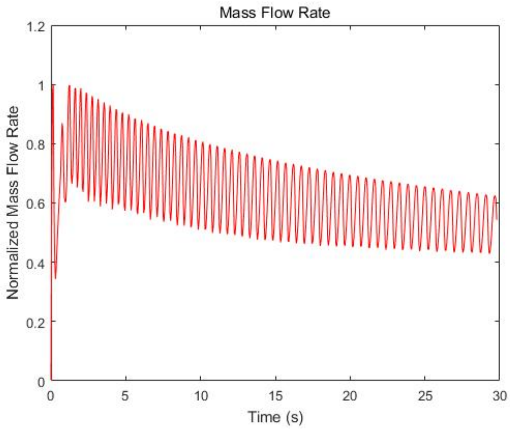

Fig.5. CFD mass flow rate without averaging

Meanwhile, if we look at the mass flow result from the CFD without any averaging over time (Fig. 5), we can clearly see some oscillation. Furthermore, the oscillation seems to be damping out very slowly. Therefore, to interpret this result and compare with the experiment, Fast Fourier Transform (FFT) was applied to both CFD results and experimental raw data.

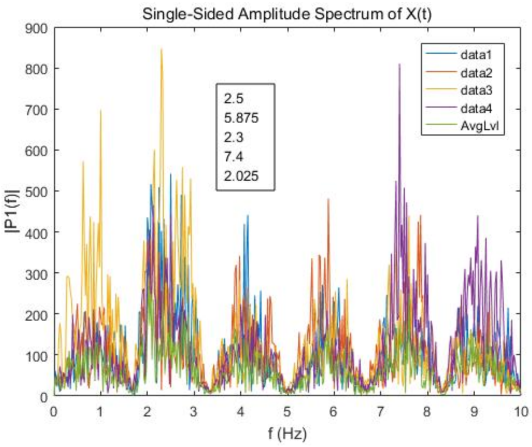

Fig.6. FFT of Experiment mass flow rate

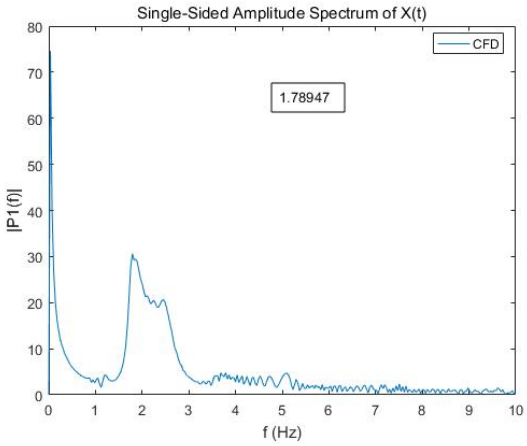

Fig.7. FFT of CFD mass flow rate

The values in the box of Fig.6. and Fig.7. shows the frequency of the peak value from the experiment and the second peak value from the CFD results respectively. We can clearly see that the first peak of oscillation in the experiment is around 2.5 Hz in Fig. 6. This matches relatively well with the frequency of 1.8 Hz from the FFT of CFD calculation. However, it is interesting to see that the higher order fluctuation is not captured in CFD. Further investigation of understanding the nature of the oscillation as well as the reason for not capturing higher order oscillation in CFD will be performed in near future.

4. Conclusions & Future Works

The safety injection tank with fluidic device was analyzed using commercial CFD. A fine resolution grid was used to capture the vortex of the fluidic device. The calculation so far has shown good consistency with the experiment. Calculation should complete by the conference date and will be thoroughly analyzed to be discussed.

Once a detailed CFD computation is finished, a small-scale experiment will be conducted for the given conditions. Using the experimental results and the CFD model, physical models can be validated to give more reliable results. The data from CFD and experiments will provide a more accurate K-factor of the fluidic device which can later be applied in system code inputs. Finally, the fluidic device design can be optimized for the future SIT designs.

ACKNOWLEDGEMENTS

Authors gratefully acknowledge that this project is funded by the KUSTAR-KAIST Institute joint research project.